Carbon and oxygen isotopic variations in early Albian limestone facies of the Mural Formation, Pitaycachi section, northeastern Sonora, Mexico

Jayagopal Madhavaraju[1,*], Alcides N. Sial[2], Carlos M. González-León[1], and Ramasamy Nagarajan[3]

[1] Estación Regional del Noroeste, Instituto de Geología, Universidad Nacional Autónoma de México, Av. L. D. Colosio s/n, esq. con Madrid, campus Universidad de Sonora, Hermosillo, Sonora 83000, México.
[2]Nucleo de Estudos Geoquímicos e Laboratório de Isótopos Estáveis (NEG - LABISE) Departmento de Geologia, Universidade Federal de Pernambuco Caixa Posta 7852, 50670-000 Recife, PE, Brazil.
[3]Department of Applied Geology, School of Engineering and Science, Curtin University, CDT 250, 98009, Miri, Sarawak, Malaysia.
**mj@geologia.unam.mx, jmadhavaraju@yahoo.com*

ABSTRACT

We used petrofacies analysis and stable isotope data to interpret the isotopic variations in the marine carbonate succession of the Early Cretaceous Mural Formation of northeastern Sonora (Pitaycachi section), Mexico. The petrographic study reveals a range of lithofacies from bioclastic mudstones to boundstones. Allochems consist of corals, algae, rudists, echinoids, sponge spicules, radiolarians, foraminifera and calpionellids. Samples analyzed for stable isotope are significantly depleted with $\delta^{18}O$ values of -15.19‰ to -6.32‰ and exhibit positive $\delta^{13}C$ values ranging from 2.91‰ to 4.39‰. The lack of correlation between $\delta^{13}C$ and $\delta^{18}O$ values also supports a primary marine origin for the $\delta^{13}C$ values of limestones from the Pitaycachi section. In the $\delta^{13}C$ profile, the Cánova Member shows an upward increasing trend from 3.09‰ to 4.36‰ interpreted to indicate an increase in the rate of marine organic production and/or organic burial in the basin during early Albian time. The abrupt increase in carbon isotope values in the lower part of the section correlates with OAE1b. The shape of the C-isotope curve of the present study is similar to other C-isotope curves from Mexico and other continents (e.g., Vacontian basin, France) indicating that OAE1b may have been global in extent.

Key words: stable isotopes, petrography, oceanic anoxic events, Pitaycachi section, Mural Formation, Sonora.

RESUMEN

En este trabajo se analizan las variaciones isotópicas en la sucesión marina carbonatada de la Formación Mural (Cretácico Inferior) que aflora en la sección Pitaycachi, noreste de Sonora, México, a partir de datos petrográficos y de isótopos estables. Las petrofacies de esta sucesión varían de "mudstone" bioclásticas a "boundstone", y los aloquímicos son corales, algas, rudistas, equinodermos, espículas de esponjas, radiolarios, foraminíferos y calpionélidos. Las calizas de la sucesión analizada por isótopos estables presentan valores bajos de $\delta^{18}O$ que varían entre -15.19‰ y -6.32‰ y valores positivos de $\delta^{13}C$ entre 2.91‰ y 4.39‰. La falta de correlación entre los valores de $\delta^{13}C$ y $\delta^{18}O$ indica un origen marino primario para los valores de $\delta^{13}C$ de las calizas de la sección de Pitaycachi. El perfil de $\delta^{13}C$ del miembro Canova de la sección estudiada muestra un incremento hacia su parte superior, que va de 3.09‰ a 4.36‰, interpretándose como un aumento en la tasa de producción de materia orgánica y/o secuestro

Madhavaraju, J., Sial, A.N., González-León, C.M., Nagarajan, R., 2013, Carbon and oxygen isotopic variations in early Albian limestone facies of the Mural Formation, Pitaycachi section, northeastern Sonora, Mexico: Revista Mexicana de Ciencias Geológicas, v. 30, núm. 3, p. 526-539.

de ella en la cuenca durante el Albiano temprano. El abrupto incremento de los valores de isótopos de carbón en la parte inferior de la sección se correlaciona con OAE1b y la forma de su curva es similar a otras reportadas de México y de otros continentes (e.g., la cuenca Vacontian en Francia), sugiriendo que OAE1b pudo haber sido un evento global.

Palabras clave: isótopos estables, petrografía, eventos anóxicos oceánicos, sección Pitaycachi, Formación Mural, Sonora.

INTRODUCTION

The carbon cycle was influenced by a series of oceanic anoxic events during the Cretaceous period and simultaneous phases of platform destruction, which are marked by several high-amplitude positive carbon isotopic excursions that have been documented globally (Jenkyns, 1995; Weissert *et al.*, 1998; Erba *et al.*, 1999; Veizer *et al.*, 1999; Herrle *et al.*, 2004; Weissert and Erba, 2004; Wissler *et al.*, 2004). An increase in atmospheric CO_2 is thought to have stimulated a global "green house" climate, which enhanced the sedimentary preservation of organic matter (increased burial) and leading to distinct Oceanic Anoxic Events (OAEs) (Schlanger and Jenkyns, 1976; Barron and Washington, 1982). Carbon isotope records are generally used to establish the global organic carbon budget during the OAEs. The significant positive carbon isotope shift that corresponds to OAE2 (Scholle and Arthur, 1980) suggests that the volume of organic carbon (C_{org}) buried was a sizable part of the global carbon budget. Isotopic studies on the shallow marine carbonates of Lower Cretaceous age have revealed evidence for paleo-oceanographic (Kumar *et al.*, 2002; Madhavaraju *et al.*, 2004; Sial *et al.*, 2001; Marquillas *et al.*, 2007; Nagarajan *et al.*, 2008; Armstrong-Altrin *et al.*, 2009), climatic and biotic changes (Deshpande *et al.*, 2003; Préat *et al.*, 2010;), in addition to global scale tectonic events (Gröcke *et al.*, 2005; Maheshwari *et al.*, 2005; Amodio *et al.*, 2008).

The sudden increase in carbon isotope values is noticed above the early Aptian (OAE1a) and remains high into Albian. The carbon isotopic variations for the Aptian-Albian interval are somewhat complex (Pratt and King, 1986) and their relationship with dysoxic/anoxic conditions (OAE1b) is less understood. In general, OAE1b includes multiple anoxic events (Jacob event, Kilian event, Paquier event and Leenhardt event) and it is also called as OAE 1b set (Föllmi *et al.*, 2006). The Albian time was characterized by a global sea level rise and geodynamic activity expressed by elevated production of oceanic crust leading to an increased rate of CO_2 degassing (Caldeira and Rampino, 1991; Larson, 1991). Major inconsistencies exist in the chronostratigraphic correlation of the carbon isotope record in the Lower Cretaceous strata of Mexico (Scholle and Arthur, 1980) and Europe (Weissert and Lini, 1991; Leckie *et al*., 2002; Herrle *et al*., 2004). Information related to the mid-Cretaceous global events is largely derived from the Tethyan sections exposed in France and Italy (Arthur and Premoli Silva, 1982; Premoli Silva *et al*., 1989; Coccioni *et al*., 1992; Herrle *et al*., 2004), whereas information on the Lower Cretaceous events exposed in Mexico is sparse (Scholle and Arthur, 1980; Bralower *et al*., 1999).

Lower Cretaceous clastic and carbonate sediments of the Bisbee Group are well exposed in Sonora, northwestern Mexico. Numerous studies (stratigraphic, palaeontological, geochemical and tectonic) have been carried out on the Mural Formation (upper Aptian-lower Albian) (Bilodeau and Lindberg, 1983; Jacques-Ayala, 1995; Lawton *et al*., 2004; González-León *et al*., 2008; Madhavaraju *et al*., 2010; Madhavaraju and González-León, 2012). However, very few published studies incorporate stable isotope data from the carbonate within the succession. Madhavaraju *et al*. (2013) carried out the carbon, oxygen and strontium isotope studies on the limestones collected from the proximal part of the Bisbee basin (Cerro Pima section) to understand the palaeoceanographic changes that occurred during the Lower Cretaceous epoch. Here we present carbon and oxygen isotope data from the more distal carbonate facies of the Bisbee basin exposed in the Cerro El Caloso-Pitaycachi section (Figure 1). The section reveals an overall shallowing-upward trend, from deep shelfal deposition in the lower part (Cánova Member) to shallow marine conditions in the upper part (El Caloso Member). Lower order shallowing-upward cycles are recognized within this overall regressive section. The objectives of the present study are: a) to provide an isotopic record of the Lower Cretaceous limestones in the distal part of the Bisbee basin; b) to assess the degree of diagenetic alteration of the isotopic signals; c) to determine the presence/absence of OAEs in the Cerro El Caloso-Pitaycachi section and: d) to compare the isotope stratigraphy of this section with that of the Cerro Pima section in western Sonora (Madhavaraju *et al.*, 2013).

GEOLOGY AND STRATIGRAPHY

Early Cretaceous sediments of the Bisbee Group are well exposed in the northern Sonora, Mexico, and show similar stratigraphic characteristics with Bisbee Group sediments exposed in southern Arizona and New Mexico, USA (Ransome, 1904; Cantú-Chapa, 1976; Bilodeau and

Figure 1. Location map of the Mural Formation in the Cerro El Caloso-Pitaycachi area.

Lindberg, 1983; Mack *et al.*, 1986; Dickinson *et al.*, 1989; Jacques-Ayala, 1995; Lawton *et al.*, 2004). The Bisbee Group is composed predominantly of sedimentary rocks with lesser amounts of volcanic deposits of Late Jurassic to Early Cretaceous age (Lawton *et al.*, 2004). In the type area (southeastern Arizona), the Bisbee Group is divided into the Glance Conglomerate, Morita Formation, Mural Formation and Cintura Formation. The Glance Conglomerate consists of cobble- to boulder-conglomerate intercalated with volcanic flows and tuffs (Bilodeau *et al.*, 1987). The Morita and Cintura Formations are dominated by fluvial siltstone, arkose and feldspathic arenite (Dickinson *et al.*, 1986; Klute, 1991). The Mural Formation however, consists of clastic and carbonate sediments that record a major marine transgression in the region of Sonora and Arizona during Aptian-Albian time (Scott, 1987).

The sedimentary sequence of the Mural Formation is well exposed in a 260 km transect from Sierra El Chanate (westernmost part) to Cerro El Caloso-Pitaycachi (northeastern most outcrops) in northern Sonora (Figure 1) (González-León *et al.*, 2008). The interpreted depositional environments of the Mural Formation vary from restricted shelf with deltaic and fluvial influence in the west to open shelf with coral rudist buildups and offshore shelf environments in the east (González-León *et al.*, 2008). A distinct lateral facies change occurs between these regions, and separate members of the Mural Formation have been recognized by Warzeski (1983, 1987) at the Sierra Anibácachi and Cerro Caloso-Cabullona localities. Warzeski (1983, 1987) recognized various members of the upper Mural Formation at the Cerro Caloso locality, namely Canova, El Caloso, La Aguja and Agua Prieta members. Outcrops of the Mural Formation at Cerro El Caloso-Pitaycahi (Figure 2) are located 30 km east of the Cerro Caloso-Cabullona but the base of the section is not exposed. The lowest exposed part below the Cánova Member consists of interbedded, green to light gray shale and siltstone with trigonids, and has been correlated with the Tuape Shale Member of this formation, which crops out to the west in northern Sonora. The ammonite *Douvilleiceras* sp. juv. cf. rex (Scott) is found in the shales of this member suggesting a latest late Aptian to early Albian age (González-León *et al.*, 2008). The Cánova member is 190 m thick and is composed of dark to light gray, thin to thick, massive to nodular limestone. The Cánova member includes Lower Albian calpionellids *Colomiella recta* and *Calpionellopsella maldonadoi*, pelagic foraminifera, notably *Globigerina* (formery *Hedbergella*) *washitensis*, sand and silt-size fragments of the pelagic crinoids *Saccocoma* sp., and also larger foraminifera such as *Orbitolina* (Warzeski, 1983).

The El Caloso member is composed of an incomplete 26 m-thick sequence that represents the lower part of this member (Warzeski, 1983 report a total thickness of 80 m for this member in Cerro Caloso-Cabullona). The El Caloso Member contains corals, algae, rudists, mollusks and larger foraminifera (*e.g.*, orbitolinids). The facies associations and faunal assemblages of the Cánova Member indicate a moderately deep to deep shelf basin, in contrast of their shallow lateral correlatives of the Los Coyotes and Cerro La Puerta members that crop out in the western part of the basin in northern Sonora. Similarly, the El Caloso member is correlative with the Cerro La Espina Member (González-León *et al.*, 2008), which represents a shallowing marine setting comprised of large patch reefs and carbonate bank complexes, following deposition of the deeper water Cánova Member.

METHODOLOGY

Twenty five thin sections were prepared for the petrographic study. Twenty one limestone samples from the Cerro El Coloso-Pitaycachi section were selected for stable isotope analysis (Figure 2). The carbon and oxygen isotope composition was analyzed using a SIRA II mass spectrometer at the Stable Isotope Laboratory (LABISE) of the Federal University of Pernambuco, Brazil. For carbon and oxygen isotope measurements, the limestone samples were treated with H_3PO_4 in a vacuum at 25 °C for one day and the resulting CO_2 gas analyzed according to the method described by Craig (1957). The evolved CO_2 gas was analyzed using the reference gas BSC (Borborema Skarn Calcite), which calibrated against NBS-18, NBS-19 and NBS-20 has a value of -11.28 ± 0.004‰ PDB for $\delta^{18}O$ and -8.58 ± 0.02‰ PDB for $\delta^{13}C$. The results are reported in the per mil notation (‰) in relation to the international VPDB scale.

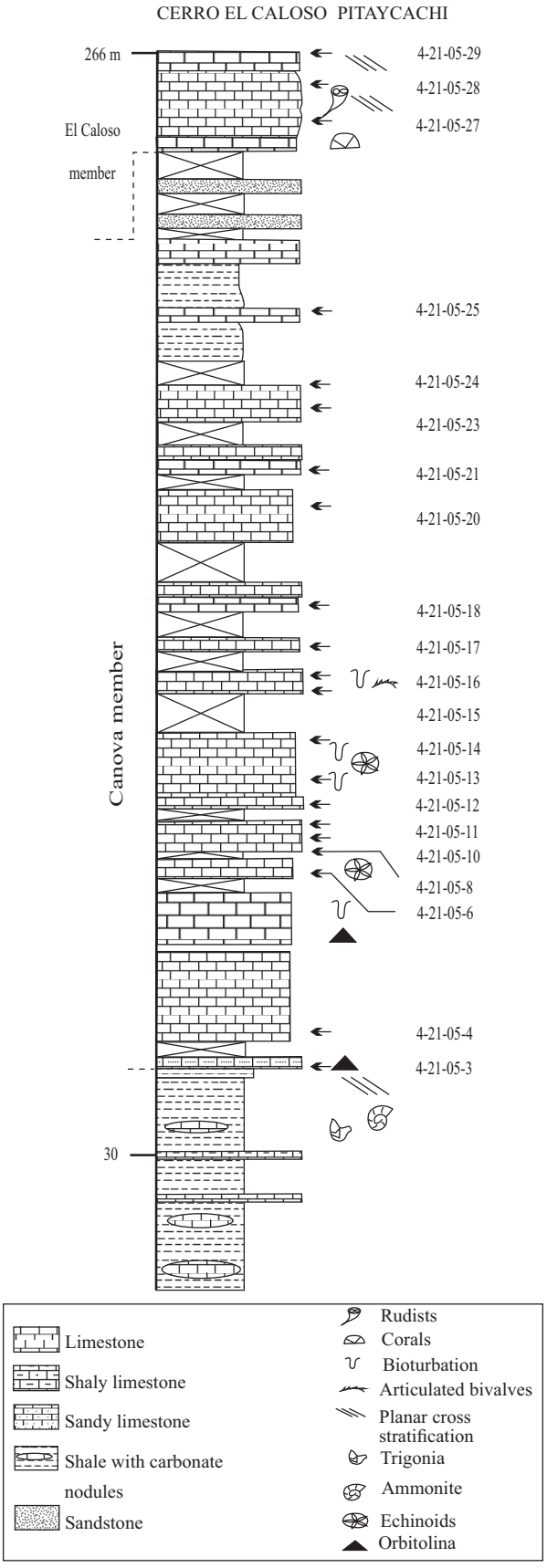

Figure 2. Lithostratigraphic section of the Mural Formation in Cerro El Caloso-Pitaycachi (modified after González-León *et al.*, 2008).

RESULTS

Petrography

Petrographic description of the carbonate samples follows the classification schemes of Dunham (1962) and the extended classification of Embry and Klovan (1971). Four major lithotypes have been identified in the Cánova and El Caloso members: i) mudstone, ii) wackestone, iii) packstone and iv) grainstone. These major lithotypes and their sub-types are discussed as follows:

Mudstone

The *Calpionellid foraminiferal mudstone* occurs in the lower and middle part of the Cánova Member and contains calpionellid, foraminifera and radiolarian grains (Figure 3a). A few sponge spicules and echinoid plates are also present in the micritic matrix. The limestone exhibits small scale veins that are filled with sparry calcite cement. Pore spaces are commonly filled with sparry and poikilotopic calcite cement.

Wackestone

Limestone beds of the lower part of the Cánova Member are characterized by the *Calpionellid wackestone* (Figure 3b). It contains predominantly calpionellids along with some foraminifera and echinoids, and minor radiolarian within the micritic matrix. The original opaline silica of the radiolarian tests have been replaced by calcite. In addition, the pore spaces present on the surface of the radiolarian test were partly replaced by micritic mud. The limestone also exhibits numerous irregular microstylolite seams. The *Echinoid foraminiferal wackestone* is present in the upper part of the Cánova Member and is characterized by echinoid and foraminiferal bioclasts within a micritic matrix (Figure 3c). Minor radiolarians and sponge spicules are found in the matrix. Also present are ferruginized intraclasts derived from the older sequence. It contains fine-grained, subangular quartz grains. Most of the quartz grains are monocrystalline, however some exhibit a polycrystalline type. Microcracks within this lithofacies are generally filled by calcite cement.

The middle part of the Cánova Member is characterized by the *Foraminiferal molluscan wackestone,* which consists of foraminifera, radiolaria and mollusks within the micritic matrix (Figures 3d, 3e). It also contains many fine- to medium-grained, subangular quartz and feldspar grains. In addition, this lithofacies contains both U and V-shaped calpionellids (Figures 3f, 3g). Many foraminiferal chambers are filled with microsparite and sparry calcite cement. Most of the quartz grains are monocrystalline with a few polycrystalline grains also present. Few echinoid spines are also seen in the micritic matrix. The limestone exhibits numerous stylolites (Figure 3h) in the foraminiferal molluscan wackestone.

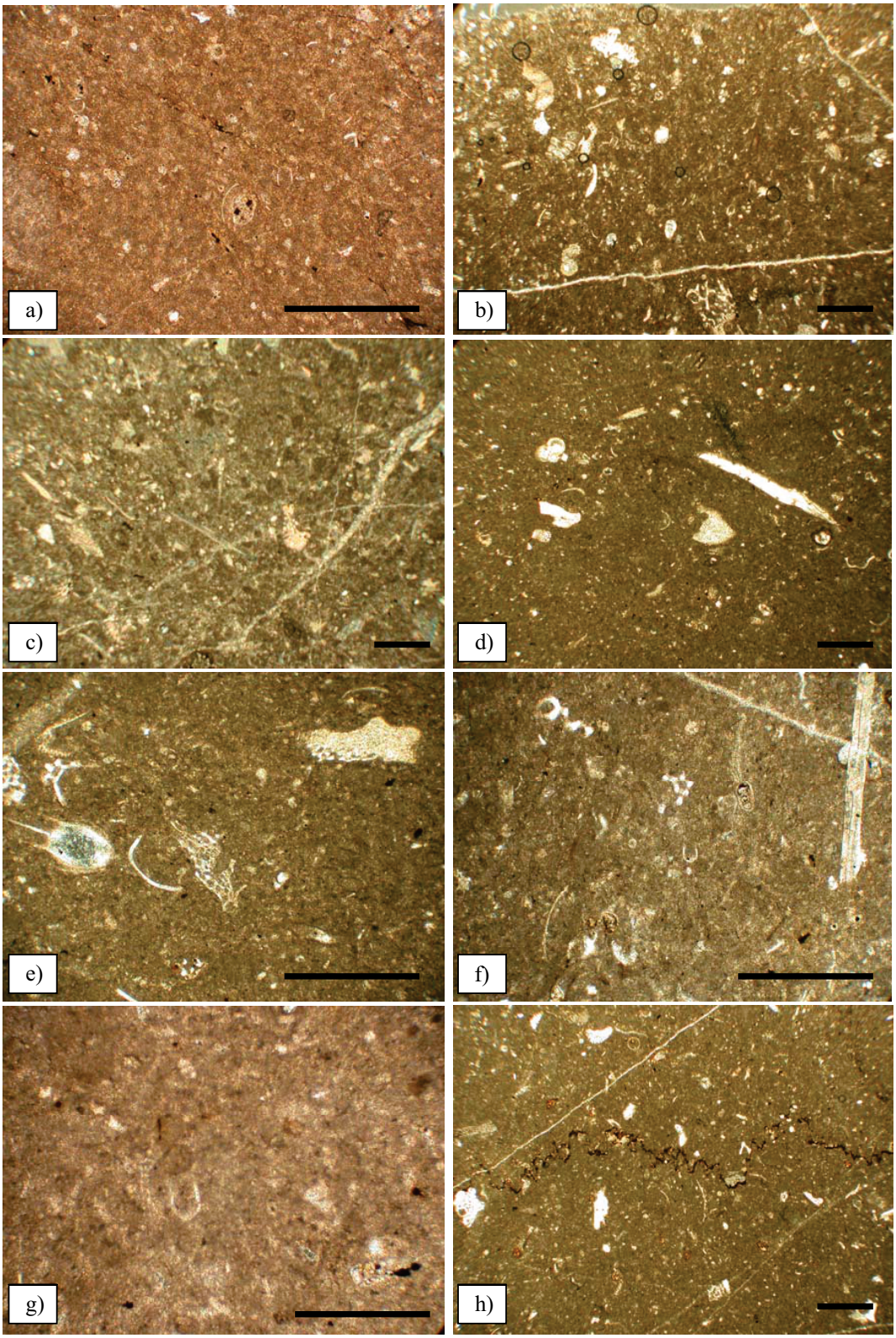

Figure 3. a) Photomicrograph showing foraminifera and calpionellid floating in micritic matrix (scale bar = 0.5 mm), b) *Calpionellid wackestone* showing calpionellids, foraminifera and echinoid grains (scale bar = 0.5 mm), c) *Echinoid foraminiferal wackestone,* with echinoid and foraminiferal bioclasts; the fractures are filled with microsparite and sparry calcite cement (scale bar = 0.5 mm), d) The limestone shows foraminifera and molluscan fragments floating in micritic matrix (scale bar = 0.5 mm), e) Photomicrograph exhibits molluscan and radiolarian grains (scale bar = 0.5 mm), f) *Foraminiferal molluscan wackestone* showing foraminifera, molluscan fragments and U-shaped calpionellids. Few reworked ferruginized grains derived from the older sequence are present as intraclasts (scale bar = 0.5 mm), g) Photomicrograph exhibits typical V-shaped calpionellids (scale bar = 0.25 mm), h) The limestone showing microstylolites and numerous dark coloured grains are concentrated along the stylolites (scale bar = 0.5 mm).

The lower part of the Cánova Member also contains the *Echinoidal foraminiferal molluscan wackestone,* which exhibits calpionellid, radiolarian, foraminifera and molluscan fragments. Echinoid plates and spines are also common in this lithofacies (Figure 4a).

Packstone

The *Coral foraminiferal molluscan packstone* is present in the upper part of the Cánova Member. It contains rudist, algae, coral, foraminifera and molluscan grains. Both planktonic and benthic foraminifera are present. Echinoid plates and spines, and some quartz grains are observed in the micritic matrix. Many foraminiferal grains are coated with a micritic layer (Figure 4b). Because of the micritic envelope, the internal structure of the shell fragments has remained intact. This lithofacies also exhibits small-scale stylolitic seams and small- to medium-scale veins filled with sparry calcite and blocky cement (Figure 4c).

Grainstone

The *Rudist foraminiferal coral grainstone,* found in the upper part of the El Caloso Member, contains rudist, foraminifera and coral framework grains (Figure 4d). Many rudist and foraminiferal grains are coated with micrite and this layer prevents the removal of the shell fragments partly or completely from this lithofacies. The limestone shows a few larger foraminifera (*e.g.*, *Mesoorbitolina)*. The primary intergranular porosity is filled by coarse sparry calcite cement. The *Foraminiferal algal coral molluscan grainstone* that is also found in the upper El Caloso Member, has a framework consisting of algae, coral, foraminifera and molluscan grains with few echinoid fragments (Figure 4e). It is also characterized by numerous, fine- to medium-grained, subangular quartz and feldspar grains. The limestone contains distinctive, large oyster shell fragments that display well defined internal layering (Figure 4f). Most of the bioclasts in this lithofacies have thin micritic coating.

Boundstone

The *Coral boundstone* has a framework comprised of molluscan and coral grains. The cross section of the corals show a cerioid growth pattern characterized by corallite which are touching each other (Figure 4g). The organic framework resulted from the complete filling of the interspaces between corallite by binding and encrusting organisms (Figure 4h). The large pore spaces between organic frameworks were partly filled with isopachous calcite cement and cavity-filling sparry calcite cement. This lithofacies also exhibits small-scale stylolites seams.

Stable isotope results

$\delta^{13}C$ and $\delta^{18}O$ values of the Cánova and El Caloso members are displayed in Table 1. The carbon isotope composition of Cánova Member ranges from 2.9‰ to 4.39‰ whereas the El Caloso member ranges from 3.11‰ to 3.64‰. Overall, limestones of the Cánova and El Caloso members show positive carbon isotope values. The Cánova Member samples show significant variation in oxygen isotope composition with values ranging from -12.23‰ to -6.32‰. The El Caloso member shows even lower oxygen isotope values that range from -15.19‰ to -12.15‰.

DISCUSSION

Lithostratigraphy and age of the Mural Formation

Most of the limestones from the Cánova Member consist of fine-grained carbonates (micrite) whereas the El Caloso Member is composed of both fine-grained (micrites) and coarse-grained carbonates (abundant bioclastic grains and coarse cements). The limestones from the lower and middle part of the Cánova Member exhibit numerous bedding-parallel, large amplitude stylolites, whereas the El Caloso Member shows a few small-scale stylolites (Figure 5a). The pressure solution effects are more prevalent in the Cánova Member and the stylolites contain numerous dark coloured insoluble materials (stylocumulate) along the pressure solution surfaces. The dark stylocumulate mainly consists of clay and pyrite. In addition, the limestone from the lower part of the Cánova Member (4-21-05-10 sample, Table 1) displays a nodular fabric that also formed due to pressure solution. The densely packed carbonate nodules are subangular with the contact between nodules often defined by dark stylolitic seams (Figure 5b).

The limestones of the Cánova Member contain a range of calpionellids. Warzeski (1987) identified *Colomiella recta* and *Calpionellopsella maldonadoi* in the Cánova Member and assigned it to the lower Albian Colomiella Zone. The *Colomiella tunisiana* and *Colomiella recta* are common in the Cánova Member and the occurrence of these species suggest placement in the Colomiella zone of Trejo (1975) (Scott, 1987). Trejo (1975) placed the Aptian-Albian boundary at the base of the *Colomiella recta* zone. Longoria (1984) proposed a detailed zonal scheme for the Cretaceous rocks exposed in the Gulf of Mexico region based on the distribution of calpionellids, nannoconids and planktonic foraminifera. He placed the Colomiella zone between K12 and K14 based on the first and last appearance of the taxa. He assigned a late Aptian – early Albian age for the Colomiella zone in agreement with Trejo (1975).

In the present study, we have identified *Colomiella recta* and *Calpionellopsella maldonadoi* species from the Cánova Member of Cerro El Caloso-Pitaycachi section. The calpionellids completely disappear in the middle part of the

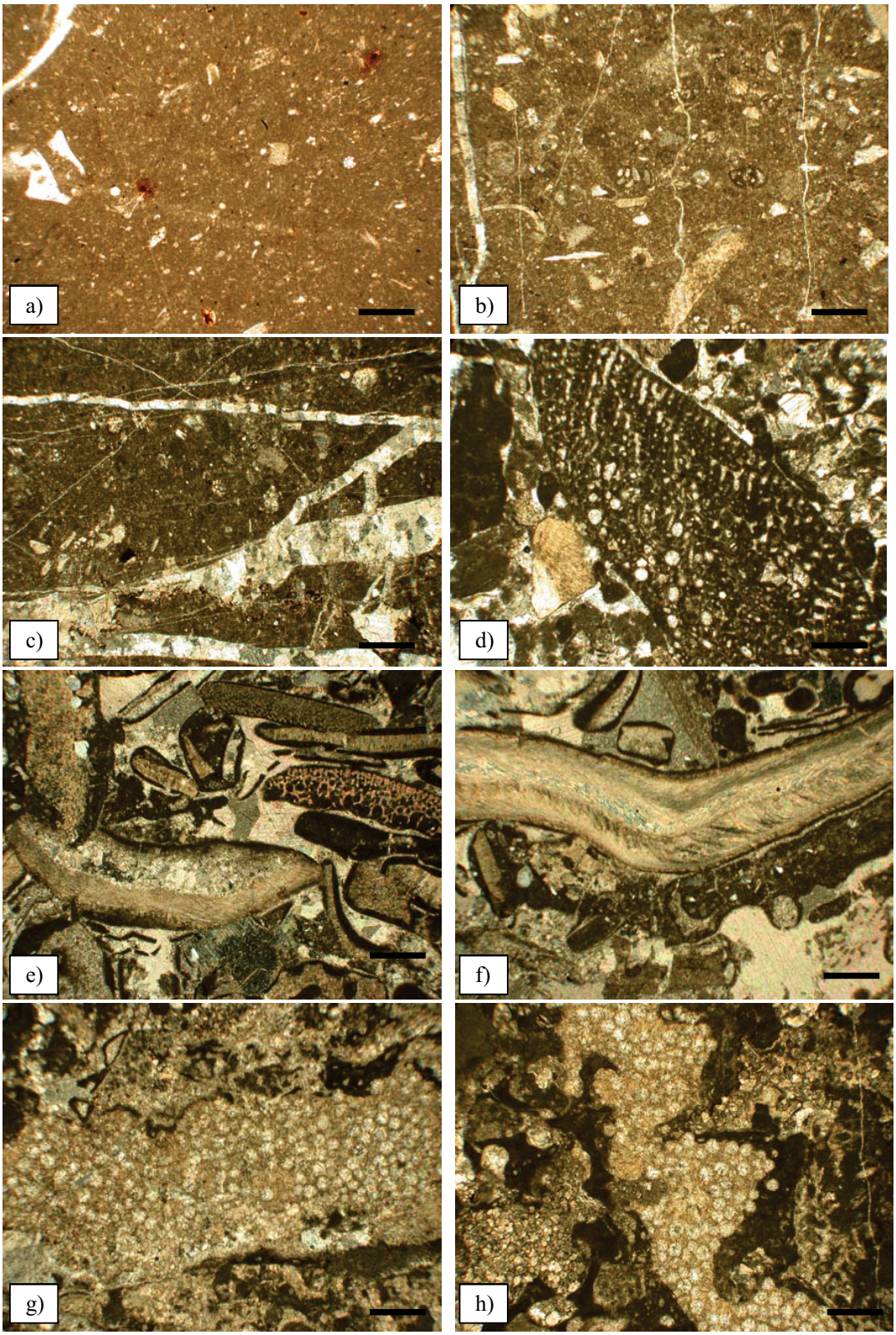

Figure 4. a) *Echinoidal foraminiferal molluscan wackestone* showing calpionellid, foraminifera, molluscan fragments along with echinoid spines (scale bar = 0.5 mm), b) Photomicrograph exhibits foraminifera, algal and molluscan grains; few subangular quartz grains are also seen (scale bar = 0.5 mm), c) Limestone showing minor and medium scale calcite veins (scale bar = 0.5 mm), d) *Rudist foraminiferal coral grainstone exhibits* framework grains include rudist, foraminifera and coral (scale bar = 0.5 mm), e) Limestone showing algal, coral and molluscan grains; most of the bioclasts are coated with micrite (scale bar = 0.5 mm), f) Photomicrograph exhibits various types of internal layers in oyster shell (scale bar = 0.5 mm), g) Limestone showing the growth pattern of corals (scale bar = 0.5 mm), h) Interspaces between corallites are bounded by encrusting organisms (scale bar = 0.5 mm).

Cánova Member (absent from sample 4-21-05-18 onwards). The common and distinctive larger foraminifera present in the Cánova Member is *Orbitolina texana* (Roemer). The presence of *Orbitolina texana* (Figure 5c) in the Cánova Member suggests that it is approximately equivalent to the lower Albian Glen Rose Formation, Texas, USA (Scott, 1987). In addition, *Globigerina* (= *Favusella*) *Washitensis* Carsey, *Globigerina planispira* Tappan and *Globigerina* (= *Hedbergella*) *delrioensis* Carsey was identified near the base of the Cánova Member in Sonora (Scott, 1987). The limestones from the El Caloso Member show rudist, coral, algal and molluscan fragments and also exhibit few larger foraminifera (*e.g.*, Orbitolina). The presence of *Calomiella recta* and *Calpionellopsella maldonadoi* in the Cánova Member also suggest an early Albian age.

Precise identification of the Aptian/Albian boundary in this section is somewhat difficult due to lack of direct age constraints. The available foraminifera and calpionellids suggest an early Albian age for the Cánova Member. The *Douvilleiceras* sp. juv. cf. rex (Scott) found below the Cánova Member suggest that its age ranges between late Aptian to early Albian (González-Léon *et al.*, 2008). In addition, the first occurrence of the Calpionellids *Colomiella recta* and *Calpionellopsella maldonadoi* occurs at the base of the Cánova Member equivalent to the lower Albian Colomiella Zone (Trejo, 1975).

Table 1. Carbon and oxygen isotopic values for whole rock limestone samples of Cerro El Caloso-Pitaycachi section of the Mural Formation.

Member/ Sample No	**$\delta^{13}C$** (‰ PDB)	**$\delta^{18}O$** (‰ PDB)
El Caloso Member		
4-21-05-29	3.32	-12.15
4-21-05-28	3.11	-15.19
4-21-05-27	3.64	-14.01
Cánova Member		
4-21-05-25	4.26	-11.94
4-21-05-24	4.38	-12.23
4-21-05-23	3.73	-11.51
4-21-05-21	4.39	-10.07
4-21-05-20	4.33	-11.35
4-21-05-18	4.36	-10.34
4-21-05-17	3.78	-8.41
4-21-05-16	3.09	-9.59
4-21-05-15	3.20	-7.58
4-21-05-14	2.98	-7.75
4-21-05-13	2.92	-7.56
4-21-05-12	2.91	-7.95
4-21-05-11	3.38	-8.11
4-21-05-10	3.37	-6.53
4-21-05-8	3.50	-6.32
4-21-05-6	2.91	-8.64
4-21-05-4	3.45	-7.69
4-21-05-3	3.37	-8.19

Identification of primary carbon isotope values

In general, marine limestones are composed of a variety of skeletal and non-skeletal grains with a certain amount of matrix material, and diagenetic processes that readily alter the primary isotopic signatures (Allan and Matthews, 1982; Veizer, 1983; Marshall, 1992; Kaufman and Knoll, 1995; Madhavaraju *et al.*, 2004; Armstrong-Altrin *et al.*, 2011). However, data from the Cánova and El Caloso members show very poor correlation between $\delta^{13}C$ and $\delta^{18}O$ values (r= -0.38, n=21; lack of statistically significant correlation; Verma, 2005, Figure 6) indicating a lack of diagenetic influence on the carbon isotopic signatures. Considering lack of correlation between $\delta^{13}C$ and $\delta^{18}O$, we suggest that limestones from the Pitaycachi section exhibit primary carbon isotope values and can be used as a direct proxy for the composition of seawater in the Bisbee basin during Aptian-Albian time.

Carbon and oxygen isotopic variations

The $\delta^{18}O$ values -in the study samples vary between -15.19‰ and -6.32‰ (Figure 7), displaying a significant decreasing upwards trend. The lower part of the Cánova Member shows comparatively heavier oxygen isotope values than the upper part and the El Caloso Member is even more ^{18}O depleted, with values ranging from -15.19 to -12.15‰. Marine limestones that have been affected by diagenesis often show more negative $\delta^{18}O$ values (Land, 1970; Allan and Matthews, 1977) because cementation and/or re-crystallization frequently takes place in fluids depleted in ^{18}O with respect to seawater (*e.g.*, meteoric water), or at elevated temperatures due to deep burials. Nevertheless, the carbon isotopes are less prone to diagenetic alterations than oxygen isotopes (Hudson, 1977; Anderson and Arthur, 1983; Banner and Hanson, 1990; Marshall, 1992; Frank *et al.*, 1999).

The carbon isotope composition of bulk carbonate shows positive $\delta^{13}C$ values throughout the study section (Figure 7). In the carbon isotope profile, the $\delta^{13}C$ value is close to 3.4‰ at the base of the section and 3.3‰ the top. The middle part of the section shows a sudden increase from 3.09‰ to 4.36‰, followed by a plateau in values, followed by a fall, rise and consistent downward trend. Such carbon isotope shifts are significant in terms of paleoceanography. According to Berger and Vincent (1986), the excess removal of 1% of the oceanic reservoir of organic carbon produces 0.2‰ of positive shift. The positive isotopic excursion observed in the middle part of the Pitaycachi section has amplitude of 1.3‰, which indicates a significant change in the carbon fluxes in the distal part of the basin during this interval. This positive $\delta^{13}C$ excursion may indicate the increasing impact of primary production in the photic zone, with associated organic burial rates exceeding those of its oxidative mineralization of organic matter (Kump and Arthur, 1999). Variations in the $\delta^{13}C$ signatures of shallow marine carbonates are widely used to interpret the primary

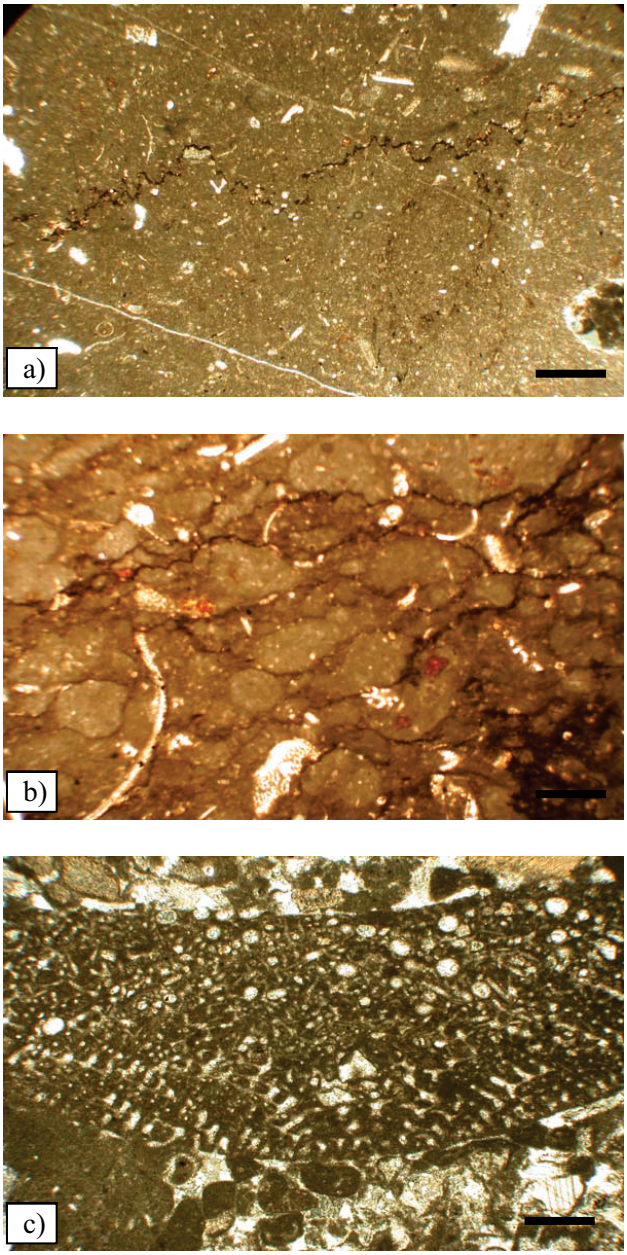

Figure 5. a) Limestone exhibit bedding parallel stylolites that contain numerous dark coloured stylocumulate along the pressure solution surfaces (scale bar = 0.5 mm), b) Photomicrograph exhibits nodular fabric (scale bar = 0.5 mm), c) Limestone showing *Orbitolina texana* along with rudist and algal fragments (scale bar = 0.5 mm).

variations in seawater $\delta^{13}C$ during the Early Cretaceous (Jenkyns, 1995; Vahrenkamp, 1996; Grötsch *et al.*, 1998). Carbon isotope values obtained from fine grained carbonate rocks are generally considered as appropriate proxies for seawater $\delta^{13}C$ because the carbon isotopic composition is more resistant to post-depositional alteration than $\delta^{18}O$ (Banner and Hanson, 1990). The limestones of the Cánova Member are fine grained (micritic) whereas those in the El Caloso Member are both fine and coarse grained. The $\delta^{13}C$ records of the Pitaycachi section suggest that the $\delta^{13}C$ values measured are considered to represent original seawater composition (mainly above 0 and below +3‰; Föllmi *et al.*, 1994). So, the carbon isotope data of bulk rocks from the Cánova and El Caloso members will be compared with the published values of late Aptian – early Albian age in order to evaluate the reliability of $\delta^{13}C$ values as a proxy for the $\delta^{13}C$ of seawater.

A number of published studies state that carbon isotope geochemistry is considered a useful tool for the interpretation of the stratigraphy of pelagic sequences (Scholle and Arthur, 1980; Schlanger *et al.*, 1987) as well as their shallow water counterparts (Jenkyns, 1995; Adabi, 1997; Ferreri *et al.*, 1997; Heldt *et al.*, 2008) and may also be used for global chronostratigraphic correlation where the age constraints are poor. The $\delta^{13}C$ values (2.91 to 4.39‰) of the analyzed samples are slightly higher than the published values thought to be typical of Albian seawater (mainly above 0 and below +3‰; Föllmi *et al.*, 1994; Menegatti *et al.*, 1998; Bralower *et al.*, 1999; Herrle *et al.*, 2004; Wissler *et al.*, 2004; Föllmi *et al.*, 2006). Although there are differences in magnitude and absolute values, the shape of the carbon isotope curve of the Cerro El Caloso-Pitaycachi section is more or less identical to those recorded in mid-Cretaceous carbonates and marlstones from Italy, Mexico, Switzerland and France (Bellanca *et al.*, 1996; Bralower *et al.*, 1999; Strasser *et al.*, 2001; Herrle *et al.*, 2003, 2004).

The carbon isotopic variations observed in the Albian interval of the Pitaycachi section ($\delta^{13}C_{carb}$ variations are ~2 per mil) are lower than the shallow water limestones of the Mural Formation in the (Cerro Pimas Section ($\delta^{13}C_{carb}$ variations are ~4 per mil). However, the magnitude of variation in $\delta^{13}C_{carb}$ values of the Pitaycachi section is similar to other Tethyan and Mexican sections (Vocontian basin, France**:** $\delta^{13}C_{carb}$ variations are ~2 per mil, after Herrle *et al.*, 2004; Mazagan Plateau**:** $\delta^{13}C_{carb}$ variations are ~2 per mil, after Herrle *et al.*, 2004; Peregrina canyon, Mexico: $\delta^{13}C_{carb}$ variations are ~2 per mil, after Scholle and Arthur, 1980).

As the Pitaycachi section was deposited in the distal part of the basin, we have compared our results with the

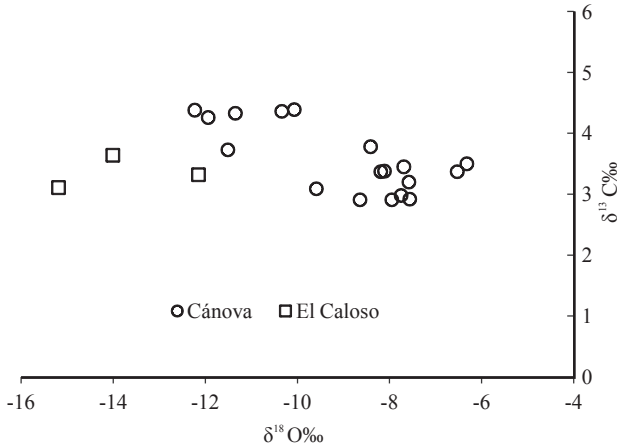

Figure 6. $\delta^{13}C$-$\delta^{18}O$ bivariate plot for limestones of the Mural Formation.

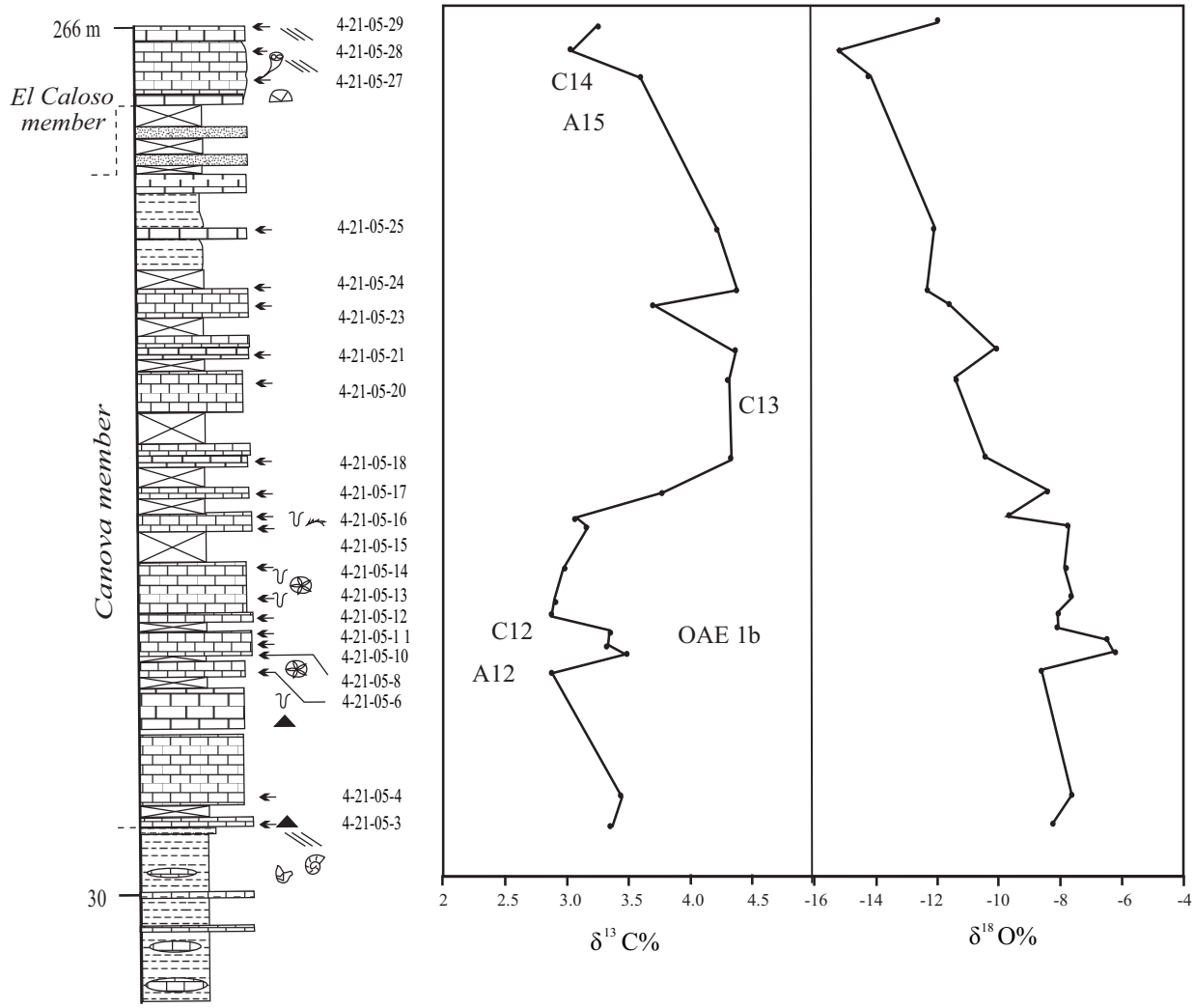

Figure 7. Carbon and oxygen isotope curves of limestones from Cerro El Caloso-Pitaycachi section, Mural Formation.

shallow water equivalent facies (Cerro Pimas section) in order to understand the lateral variations in the isotopic shift. The deep water Cánova Member is correlatable with the shallow facies equivalent of the Los Coyotes and Cerro La Puerta members, while the El Caloso Member is correlated with the Cerro La Espina Member (González-Léon *et al.*, 2008). The limestones from the Los Coyotes and Cerro La Espina members are well developed in the Cerro Pimas section and the carbon isotope curve for this section has been studied by Madhavaraju *et al.* (2013). The carbon isotope curve in the Cerro Pimas section (-2.5 to +2.2‰ VPDB) shows fluctuations with larger amplitude than observed in the C-isotopic curve of the Pitaycachi section (+2.91 to +4.39‰ VPDB). It suggests that the shallow water settings are comparatively less stable in their isotopic composition than the open marine settings and that numerous factors, including changes in productivity, may magnify changes of the global oceanic carbon reservoir (Jenkyns, 1995; Vahrenkamp, 1996; Wissler *et al.*, 2004). Overall, the carbon isotope curve of the Pitaycachi section is comparable to that of the Cerro Pimas section of the Mural Formation. We also compared the carbon isotope curve of the Pitaycachi section with those of Scholle and Arthur (1980) and Herrle *et al.* (2004) curves to understand the similarities between them (Figure 8). Based on the published isotope curves, we have identified three comparable segments (C12, C13 and C14) of Bralower *et al.* (1999) isotope curve and two identical segments (Al2 and Al5) of Herrle *et al.* (2004) curve.

In the Pitaycachi section, the commencement of OAE1b is coincident with a sharp positive $\delta^{13}C$ excursion followed by a decrease in $\delta^{13}C$ values. The present study suggests that the global OAE1b is also present in the distal part of the Bisbee basin recorded in the Pitaycachi section. Although, as correlated, the Pitaycachi section has a significant positive excursion above OAE1b (Paquier event), which suggests that the Bisbee basin might have been ex-

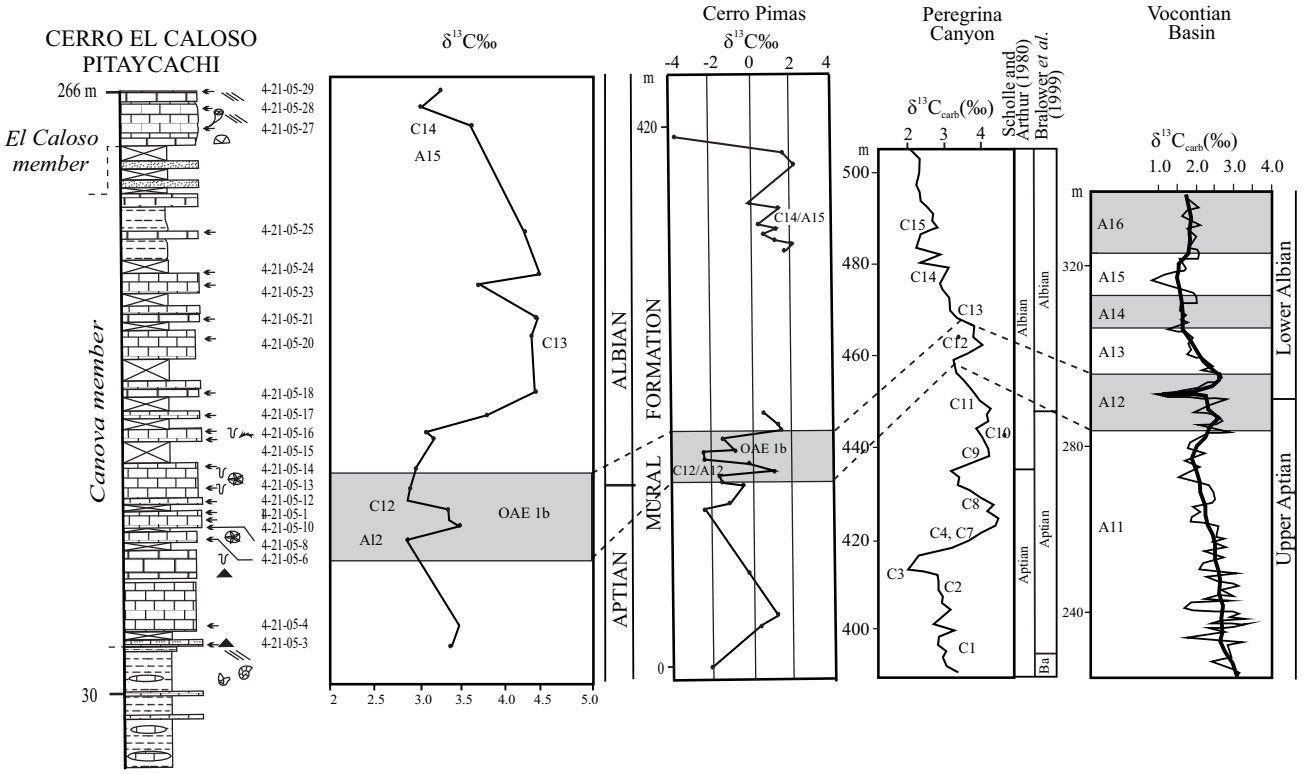

Figure 8. Carbon isotope curve of the present study compared with Cerro Pimas section, Mexico (Madhavaraju *et al.*, 2013), Peregrina canyon, Mexico (Scholle and Arthur, 1980; Bralower *et al.*, 1999) and Vocontian basin, France (Herrle *et al.*, 2004).

perienced multiple anoxic events (OAE 1b set) during the early Albian time. The observed OAE1b in this section may be comparable to Paquier event. Further, the detailed and high-resolution isotopic study in this section will provide further clue regarding the presence of other anoxic event particularly Leenhardt event.

CONCLUSIONS

The limestones of Cánova Member mainly consist of micrite whereas the El Caloso member contains both micrite and coarse grained carbonate (more sparry calcite and blocky cements). The presence of the calpionellid species *Calomiella recta* and *Calpionellopsella maldonadoi,* and larger foraminifera like *Orbitolina texana* in the Cánova Member suggest an early Albian age. The limestones show more negative $\delta^{18}O$ values (-15.19‰ to -6.32‰) where as $\delta^{13}C$ values show significant positive values (2.91‰ to 4.39‰). The lack of correlation between $\delta^{18}O$ and $\delta^{13}C$ values suggests that the limestones were not subjected to significant post-depositional modification and preserve their primary carbon isotope signatures. The carbon isotope curve of the present study shares three comparable segments (C12, C13 and C14) with that published by Bralower *et al.* (1999), and two identical segments (Al2 and Al5) with the Herrle *et al.* (2004) curve. The onset of OAE1b is paralleled by a significant increase in $\delta^{13}C$ values in the Pitaycachi section, and is followed by a negative excursion. The general patterns of $\delta^{13}C$ values excursions in the study section can be correlated with other Mexican and Tethyan sections.

ACKNOWLEDGEMENTS

This work was supported by Dirección General de Asuntos del Personal Académico, Universidad Nacional Autónoma de Mexico (UNAM) through Programa de Apoyo para la Superación del Personal Académico de la UNAM. We would like to thank Dr. Jonathan Kiddings and Dr. J.S. Armstrong-Altrin for their useful comments and suggestions which improved the quality of this paper. We thank Mr. Pablo Peñaflor, Estación Regional del Noroeste, Instituto de Geología, Universidad Nacional Autónoma de México for powdering of limestone samples for isotope analyses. We also thank Mrs. Adriana Aimée Orcí Romero for preparing thin sections for the petrographic study.

REFERENCES

Adabi, M.H., 1997, Application of carbon isotope chemostratigraphy to the Renison dolomites, Tasmania: a Neoproterozoic age: Australian Journal of Earth Sciences, 44, 767-775.

Allan, J.R., Matthews, R.K., 1977, Carbon and oxygen isotopes as diagenetic and stratigraphic tools: data from surface and subsurface of Barbados, West Indies: Geology, 5, 16-20.

Allan, J.R., Matthews, R.K., 1982, Isotope signatures associated with early meteoric diagenesis: Sedimentology, 29, 797-817.

Amodio, S., Ferreri, V., D'Argenio, B., Weissert, H., Sprovieri, M., 2008, Carbon-isotope stratigraphy and cyclostratigraphy of shallow-marine carbonates: the case of San Lorenzello, Lower Cretaceous of southern Italy: Cretaceous Research, 29(5-6), 803-813.

Anderson, T.F., Arthur, M.A., 1983, Stable isotopes of oxygen and carbon and their application to sedimentologic and paleoenvironmental problems, *in* Arthur, M.A., Anderson, T.F., Kaplan, I.R., Veizer, J., Land, L.S. (eds.), Stable Isotopes in Sedimentary Geology: Society of Economic Paleontologists and Mineralogists, Short Course Notes, 10, 1-151.

Armstrong-Altrin, J.S., Madhavaraju, J., Sial, A.N., Kasper-Zubillaga, J.J., Nagarajan, R., Flores-Castro, K., Rodríguez, J.L., 2011, Petrography and stable isotope geochemistry of the Cretaceous El Abra Limestones (Actopan), Mexico: Implication on diagenesis: Journal of the Geological Society of India, 77(4), 349-359.

Armstong-Altrin, J.S., Lee, Y.I., Verma, S.P., Worden, R.H., 2009, Carbon, oxygen and strontium isotope geochemistry of carbonate rocks of the upper Miocene Kudankulam Formation, southern India: Implications for paleoenvironment and diagenesis: Chemie der Erde, 69, 45-60.

Arthur, M.A., Premoli Silva, I., 1982, Development of wide-spread organic carbon-rich strata in Mediterranean Tethys, *in* Schlanger, S.O. Cita, M.B. (eds.), Nature and Origin of Cretaceous Carbon-rich Facies: London, Academic Press, 7-54.

Banner, J.L., Hanson, G.N., 1990, Calculation of simultaneous isotopic and trace element variations during water-rock interaction with applications to carbonate diagenesis: Geochimica et Cosmochimica Acta, 54, 3123-3137.

Barron, E.J., Washington, W.M., 1982, Cretaceous climate: a comparison of atmospheric simulations with the geologic record: Palaeogeography, Palaeoclimatology, Palaeoecology, 40, 103-133.

Bellanca, A., Claps, M., Erba, E., Masetti, D., Neri, R., Premoli Silva, I., Venecia, F., 1996, Orbitally induced limestone/marlstone rhythms in the Albian-Cenomanian Cismon section (Venetian region, northern Italy): sedimentology, calcareous and siliceous plankton distribution, elemental and isotope geochemistry: Palaeogeography, Palaeoclimatology, Palaeoecology, 126, 227-260.

Berger, W.H., Vincent, E., 1986, Deep sea carbonates: reading the carbon isotope signal: Geologische Rundschau, 75, 249-269.

Bilodeau, W.L., Linberg, F.A., 1983, Early Cretaceous tectonics and sedimentation in southern Arizona, southwestern New Mexico, and northern Sonora, Mexico, *in* Reynolds, M.W., Dolly, E.D., (eds.), Mesozoic paleogeography of West-Central United States: Society of Economic Paleontologists and Mineralogists, Rocky Mountain Section, Rocky Mountain Paleogeography Symposium, 2, 173-188.

Bilodeau, W.L., Kluth, C.F., Vedder, L.K., 1987, Regional stratigraphic, sedimentologic, and tectonic relationships of the Glance Conglomerate in southeastern Arizona, *in* Dickinson, W.R., Klute, M.F. (eds.), Mesozoic rocks of southern Arizona adjacent areas: Arizona Geological Society Digest, 18, 229–256.

Bralower, T.J., Cobabe, E., Clement, B., Sliter, W.V., Osburn, C.L., Longoria, J., 1999, The record of global change in mid-Cretaceous (Barremian-Albian) sections from the Sierra Madre, Northeastern Mexico: Journal of Foraminiferal Research, 29, 418-437.

Caldeira, K., Rampino, M.R., 1991, The mid-Cretaceous super plume, carbon dioxide, and global warming: Geophysical Research Letters, 18, 987-990.

Cantú-Chapa, A., 1976, Nuevas localidades del Kimeridgiano y Titoniano en Chihuahua (Norte de México): Revista del Instituto Mexicano del Petróleo, 7, 38-45.

Craig, H., 1957, Isotopic standards for carbon and oxygen and correction factors for mass spectrometric analyses of carbon dioxide: Geochimica et Cosmochimica Acta, 12, 133-149.

Coccioni, R., Erba, E., Premoli Silva, I., 1992, Barremian-Aptian calcareous plankton biostratigraphy from Gorgo Cerbara section (Marche, Central Italy) and implications for plankton evolution: Cretaceous Research, 13, 517-537.

Deshpande, R.D., Bhattacharya, S.K., Jani, R.A., Gupta, S.K., 2003, Distribution of oxygen and hydrogen isotopes in shallow ground waters from southern India: influence of a dual monsoon system: Journal of Hydrology, 271, 226-239.

Dickinson, W.R., Klute, M.A., Swift, P.A., 1986, The Bisbee Basin and its bearing on late Mesozoic paleogeographic and plate tectonic relations between the Cordilleran and Caribean regions, *in* Abbott, P.L. (ed.), Cretaceous Stratigraphy, Western North America, Pacific Section: Society for Sedimentary Geology, Society of Economic Paleontologists and Mineralogists Book, 46, 51-62.

Dickinson, W.R., Klute, M.A., Swift, P.A., 1989, Cretaceous strata of southern Arizona, *in* Jenney, J.P., Reynols, S.J. (eds.), Geologic Evolution of Arizona: Arizona Geological Society Digest, 17, 447-462.

Dunham, R.J., 1962, Classification of carbonate rocks according to depositional texture, *in* Ham, W.E. (ed.), Classification of carbonate rocks: American Association of Petroleum Geologists Memoir, 108-121.

Embry, A.F., Klovan, J.E., 1971, A Late Devonian reef tract on northeastern Flanks Island, Nothwest Territories: Canadian Petroleum Geology Bulletin, 19, 730-781.

Erba, E., Channell, J.E.T., Claps, M., Jones, C., Larson, R., Opdyke, B., Silva, I.P., Riva, A., Salvini, G., Torricelli, S., 1999, Integrated stratigraphy of the Cismon APTICORE (Southern Alps, Italy): A "reference section" for the Barremian-Aptian interval at low latitudes: Journal of Foraminiferal Research, 29, 371-391.

Ferreri, V., Weissert, H., D´Argenio, B., Buonocunto, P., 1997, Carbon isotope stratigraphy: A tool for basin to carbonate platform correlation: Terra Nova, 9, 57-61.

Föllmi, K.B.,Weissert, H., Bisping, M. Funk, H., 1994, Phosphogenesis, carbon-isotope stratigraphy, and carbonate-platform evolution along the Lower Cretaceous northern Tethyan margin: Geological Society of America Bulletin, 106(6), 729-746.

Föllmi, K.B., Godet, A., Bodin, S., Linder, P., 2006, Interaction between environmental change and shallow water carbonate buildup along the northern Tethyan margin and their impact on the Early Cretaceous carbon isotope record: Paleoceanography, 21, 1-16.

Frank, T.D., Arthur, M.A., Dean, W.E., 1999, Diagenesis of Lower Cretaceous pelagic carbonates, North Atlantic: paleoceanographic signals obscured: Journal of Foraminiferal Research, 29, 340-351.

González-León, C.M., Scott, R.W., Loser, H., Lawton, T.F., Robert, E., Valencia, V.A., 2008, Upper Aptian-Lower Albian Mural Formation: stratigraphy, biostratigraphy and depositional cycles on the Sonoran shelf, northern Mexico: Cretaceous Research, 29, 249-266.

Gröcke, D.R., Price, G.D., Robison, S.A., Baraboshkin, E.Y., Mutterlose, J., Ruffell, A.H., 2005, The Upper Valanginian (Early Cretaceous) positive carbon-isotope event recorded in terrestrial plants: Earth and Planetary Science Letters, 240(2), 495-509.

Grötsch, J., Billing, I., Vahrenkamp, V., 1998, Carbon-isotope stratigraphy in shallow water carbonates: implications for Cretaceous black-shale deposition: Sedimentology, 45(4), 623-634.

Heldt, M., Bachmann, M., Lehmann, J., 2008, Microfacies, biostratigraphy, and geochemistry of the hemipelagic Barremian-Aptian in north-central Tunisia: influence of the OAE1a on the southern Tethys margin: Palaeogeography, Palaeoclimatology, Palaeoecology, 235, 93-109.

Herrle, J.O., Pross, J., Friedrich, O., Erlenkeuser, H., Kossler, P., Hemleben, C., 2003, Forcing mechanisms for mid-Cretaceous black shale formation: Evidence from the upper Aptian and lower Albian of the Vocontian Basin (SE France): Palaeogeography, Palaeoclimatology, Palaeoecology, 190, 399-426.

Herrle, J.O., Kobler, P., Friedrich, O., Erlenkeuser, H., Hemleben, C., 2004, High-resolution carbon isotope records of the Aptian to Lower Albian from SE France and the Mazagan Plateau (DSDP Site 545): a stratigraphic tool for paleoceanographic and paleobiologic reconstruction: Earth and Planetary Science Letters, 218, 149-161.

Hudson, J.D., 1977, Stable isotopes and limestone lithification: Journal of the Geological Society, London, 133(6), 637-660.

Jacques-Ayala, C., 1995, Paleogeography and provenance of the Lower Cretaceous Bisbee Group in the Caborca-Santa Ana area, northwestern Sonora, *in* Jacques-Ayala, C., González-León, C.M., Roldán-Quintana, J. (eds.), Studies on the Mesozoic of Sonora and adjacent areas: Geological Society of America Special Paper, 301, 79-98.

Jenkyns, H.C., 1995, Carbon isotope stratigraphy and paleoceanographic significance of the Lower Cretaceous shallow-water carbonates of Resolution Guyot, Mid-Pacific Mountains: Proceedings of Ocean Drilling Program, Scientific Results, 143, 99-104.

Kaufman, A.J., Knoll, A.H., 1995, Neoproterozoic variations in the C-isotopic composition of seawater: stratigraphic and biogeochemical implications: Precambrian Research, 73(1-4), 27-49.

Klute, M.A., 1991, Sedimentology, sandstone petrofacies, and tectonic setting of the late Mesozoic Bisbee basin, southeastern Arizona: Tucson, Arizona, University of Arizona, doctoral dissertation, 268 pp.

Kumar, B., Sharma, S.D., Sreenivas, B., Dayal, A.M., Rao, M.N., Dubey, N., Chawla, B.R., 2002, Carbon, oxygen and strontium isotope geochemistry of Proterozoic carbonate rocks of the Vindhyan Basin, central India: Precambrian Research, 113, 43-63.

Kump, L.R., Arthur, M.A., 1999, Interpreting carbon-isotope excursions: carbonates and organic matter: Chemical Geology, 161, 181-198.

Land, L.S., 1970, Phreatic versus vadose meteoric diagenesis of limestones: evidence from a fossil water table: Sedimentology, 14, 175-185.

Larson, R.L., 1991, Latest pulse of the Earth: evidence for a mid-Cretaceous super plume: Geology, 19, 547-550.

Lawton, T.F., González-León, C.M., Lucas, S.G., Scott, R.W., 2004, Stratigraphy and sedimentology of the Upper Aptian-upper Albian Mural Limestone (Bisbee Group) in northern Sonora, Mexico: Cretaceous Research, 25, 43-60.

Leckie, R.M., Bralower, T.J., Cashman, R., 2002, Oceanic anoxic events and plankton evolution: Biotic response to tectonic forcing during the mid-Cretaceous: Paleoceanography, 17, 10.1029/201PA000623.

Longoria, J.F., 1984, Cretaceous biochronology from the Gulf of Mexico region based on planktonic microfossils: Micropaleontology, 30, 225-242.

Mack, G.H., Kolins, W.B., Galemore, J.A., 1986, Lower Cretaceous stratigraphy, depositional environments, and sediment dispersal in southwestern New Mexico: American Journal of Science, 286, 309-331.

Madhavaraju, J., González-León, C.M., 2012, Depositional conditions and source of rare earth elements in carbonate strata of the Aptian-Albian Mural Formation, Pitaycachi section, northeastern Sonora, Mexico: Revista Mexicana de Ciencias Geológicas, 29(2), 478-491.

Madhavaraju, J., Kolosov, I., Buhlak, D., Armstrong-Altrin, J.S., Ramasamy, S., Mohan, S.P., 2004, Carbon and oxygen isotopic signatures in Albian-Danian limestones of Cauvery basin, southeastern India: Gondwana Research, 7(2), 527-537.

Madhavaraju, J., González-León, C.M., Lee, Y.I., Armstrong-Altrin, J.S., Reyes Campero, L.M., 2010, Geochemistry of the Mural Formation (Aptian-Albian) of the Bisbee Group, Northern Sonora, Mexico: Cretaceous Research, 31, 400-414.

Madhavaraju, J., Lee, Y.I., González-León, C.M., 2013, Diagenetic significance of carbon, oxygen and strontium isotopic compositions in the Aptian-Albian Mural Formation in Cerro Pimas area, northern Sonora, Mexico: Journal of Iberian Geology, 39(1), 73-88.

Maheshwari, A., Sial, A.N., Guhey, R., Ferreira, V.P., 2005, C-isotope composition of carbonates from Indravati Basin, India: Implications for regional stratigraphic correlation: Gondwana Research, 8(4), 603-610.

Marquillas, R., Sabino, I., Sial, A.N., del Papa, C., Ferreira, V., Matthews, S., 2007, Carbon and oxygen isotopes of Maastrichtian-Danian shallow marine carbonates: Yacoraite Formation, northwestern Argentina: Journal of South American Earth Sciences, 23, 304-320.

Marshall, J.D., 1992, Climatic and oceanographic isotopic signals from the carbonate rock record and their preservation: Geological Magazine, 129, 143-160.

Menegatti, A.P., Weissert, H., Brown, R.S., Tyson, R.V., Farrimond, P., Strasser, A., Caron, M., 1998, High-resolution $\delta^{13}C$ stratigraphy through the early Aptian "Livello Selli" of the Alpine Tethys: Paleoceanography, 13, 530-545.

Nagarajan, R. Sial, A.N., Armstrong-Altrin, J.S., Madhavaraju, J., Nagendra, R., 2008, Carbon and oxygen isotope geochemistry of Neoproterozoic limestones of the Shahabad Formation, Bhima Basin, Karnataka, southern India: Revista Mexica de Ciencias Geologicas, 25(2), 225-235.

Pratt, L.M., King, J.D., 1986, Low marine productivity and high eolian input recorded by rhythmic black shales in mid-Cretaceous pelagic deposits from Central Italy: Paleoceanography, 1, 507-522.

Préat, A., Kolo, K., Prian, J-P., Delpomdor, F., 2010, A peritidal evaporite environment in the Neoproterozoic of South Gabon (Schisto-Calcaire Subgroup, Nyanga Basin): Precambrian Research, 177(3-4), 253-265.

Premoli Silva, I., Erba, E., Tornaghi, M.E., 1989, Paleoenvironmental signals and changes in surface fertility in mid-Cretaceous Corg-rich pelagic facies of the fucoid mares (central Italy): Geobios Memoir Special, 11, 225-236.

Ransome, F.L., 1904, The geology and ore deposits of the Bisbee quadrangle Arizona: United States Geological Survey, Professional Paper 21, 167 p.

Schlanger, S.O., Jenkyns, H.C., 1976, Cretaceous oceanic anoxic events: causes and consequences: Geologie en Mijnbouw, 55, 179-184.

Schlanger, S.O., Arthur, M.A., Jenkyns, H.C., Scholle, P.A., 1987, The Cenomanian-Turonian oceanic anoxic event, I. Stratigraphy and distribution of organic carbon-rich beds and marine $\delta^{13}C$ excursion, *in* Brooks, J., Fleet, A. (eds.), Marine Petroleum Source Rocks: Geological Society, London, Special Publication 24, 347-375.

Scholle, P.A., Arthur, M.A., 1980, Carbon isotope fluctuations in Cretaceous pelagic limestones: Potential stratigraphic and petroleum exploration tool: Bulletin of the American Association of Petroleum Geologists, 64, 67-87.

Scott, R.W., 1987, Stratigraphy and correlation of the Cretaceous Mural Limestone, Arizona and Sonora, *in* Dickinson, W.R., Klute, M.F., (eds.), Mesozoic rocks of Southern Arizona adjacent areas: Arizona Geological Society Digest, 18, 327-334.

Sial, A.N., Ferreira, V.P., Toselli, A.J., Parada, M.A., Aceñolaza, F.G., Pimentel. M.M., Alonso, R.N., 2001, Carbon and oxygen isotope composition of some Upper Cretaceous-Paleocene sequences in Argentina and Chile: International Geology Review, 43, 892-909.

Strasser, A., Caron, M., Gjermeni, M., 2001, The Aptian, Albian and Cenomanian of Roter Sattel, Romandes Prealps, Switzerland: a high resolution record of oceanographic changes: Cretaceous Research, 22, 183-199.

Trejo, M., 1975, Zonificacion del límite Aptiano-Albiano de México: Revista del Instituto de Mexicano Petróleo, 7, 6-29.

Vahrenkamp, V.C., 1996, Carbon isotope stratigraphy of the Upper Kharaib and Shuaiba Formations: implications for the Lower Cretaceous evolution of the Arabian Gulf Region: American Association of Petroleum Geologists Bulletin, 80, 647-62.

Veizer, J., 1983, Chemical diagenesis of carbonates; theory and application of trace element technique, *in* Arthur, M.A., Anderson, T.F., Kaplan, I.R., Veizer, J., Land, L.S. (eds.), Stable Isotopes in Sedimentary Geology: Society of Economic Palaeontologists and Mineralogists, Short Course 10, 3-100.

Veizer, J., Ala, D., Azmy, K., Bruckschen, P., Buhl, D., Bruhn, F.,Carden, G.A.F., Diener, A., Ebneth, S., Goddéris, Y., Jasper, T., Korte, C., Pawellek, F., Podlaha, O.G., Strauss, H., 1999, $^{87}Sr/^{86}Sr$, $\delta^{13}C$ and $\delta^{18}O$ evolution of Phanerozoic seawater: Chemical Geology, 161, 59-88.

Verma, S.P., 2005, Estadística básica para el manejo de datos experimentales: Aplicación en la geoquímica (geoquimiometría): Mexico, D.F., Universidad Nacional Autónoma de México, 186 pp.

Warzeski, E.R., 1983, Facies patterns and diagenesis of a Lower Cretaceous carbonate shelf, norhteastern Sonora and southeastern Arizona:

Binghampton, New York, New York State University, doctoral dissertation, 401 pp.

Warzeski, E.R., 1987, Revised stratigraphy of the Mural Limestone: A Lower Cretaceous carbonate shelf in Arizona and Sonora, *in* Dickinson, W.R., Klute, M.F. (eds.), Mesozoic rocks of Southern Arizona adjacent areas: Arizona Geological Society Digest, 18, 335-363.

Weissert, H., Erba, E., 2004, Volcanism, CO_2 and palaeoclimate: a Late Jurassic–Early Cretaceous carbon and oxygen isotope record: Journal of the Geological Society, London, 161(4), 695-702.

Weissert, H., Lini, A., 1991, Ice age interludes during the time of Cretaceous greenhouse climate?, *in* Müller, D.W., McKenzie, J.A.,Weissert, H. (eds.), Controversies in Modern Geology; Evolution of Geologic Theories in Sedimentology, Earth History and Tectonics: New York, Academic Press, 173-191.

Weissert, H., Lini, A., Föllmi, K.B., Kuhn, O., 1998, Correlation of Early Cretaceous carbon isotope stratigraphy and platform drowning events: a possible link?: Palaeogeography, Palaeoclimatology, Palaeoecology, 137, 189-203.

Wissler, L., Weissert, H., Buonocunto, F.P., Ferreri, V., D´Argenio, B., 2004, Calibration of the Early Cretaceous time scale: a combined chemostratigraphic and cyclostratigraphic approach to the Barremian-Aptian interval, *in* D´Argenio, B., Fischer, A.G., Premoli Silva, I., Weissert, H., Ferreri, V. (eds.), Cyclostratigraphy, Approaches and case histories: Society for Sedimentary Geology, SEPM Special Publication, 81, 123-134.

Manuscript received: July 27, 2012
Corrected manuscript received: September 20, 2013
Manuscript accepted: September 23, 2013